SCREW-GLUING OF RIBBED TIMBER ELEMENTS – EFFECTS OF SCREW SPACING AND PLATE STIFFNESS ON BOND LINE CRAMPING PRESSURE

SCHRAUBENPRESSKLEBUNG VON HOLZRIPPEN-ELEMENTEN – EINFLUSS DES SCHRAUBENABSTANDES UND DER PLATTENSTEIFIGKEIT AUF DEN KLEBFUGEN-PRESSDRUCK

Simon Aicher, Nikola Zisi, Kai Simon

Materials Testing Institute (MPA), University of Stuttgart, Otto-Graf-Institute

SUMMARY

The paper reports on cramping pressure distribution at screw-gluing of ribbed timber elements. The cramping pressure is exerted and limited by the head pull-through capacity of partially threaded self-tapping screws. The regarded deck plates and ribs consist of cross laminated timber (CLT) and glued laminated timber (GLT), respectively. The investigated plate thicknesses range from 60 mm to 200 mm and hence exceed the presently permissible 50 mm specified in the relevant German standard DIN 1052-10 [12] partly in very pronounced manner. The numerical finite element investigations aimed at the interacting effects of screw spacing and of the bending stiffness of the plate on the cramping pressure. Further the preferability of a staggered vs. a not staggered placement of the screws in multi-row applications was regarded.

The cramping pressure variation within the nominal influence area of a screw increases in extreme manner with thinner, less bending stiff plates and larger screw spacings. These findings, being in line with point loaded beams and plates on elastic foundation were captured quantitatively for a wide range of geometry and stiffness configurations. Based hereon a new cramping pressure verification is proposed which addresses averaged compressive stresses of low-pressure areas within the nominal screw cramping influence area. The resistance side is then regarded, different from ÖNORM B 1995-1-1 [14], as an intrinsic material, i.e. adhesive property, which is independent from the specific geometric screw-gluing configuration. Within the investigated boundaries of plate stiffnesses and screw

spacings a staggered screw placement produced smaller locally confined low cramping pressure areas and hence is preferable in multi-row screw applications, necessary at larger rib widths.

ZUSAMMENFASSUNG

Der Beitrag berichtet über die Pressdruckverteilung bei der Schraubenpressklebung von Holzrippenelementen. Der Pressdruck wird durch die Kopfdurchzieh-Tragfähigkeit der Schraube ausgeübt und beschränkt. Die betrachteten (Deck-) Platten und die Rippen bestehen aus Brettsperrholz (BSP) und Brettschichtholz (BSH). Die im Speziellen untersuchten Plattendicken umfassen 60 mm bis 200 mm und überschreiten somit die heute in der relevanten deutschen Norm DIN 1052-10 [12] zulässigen Abmessungen teilweise wesentlich. Die numerischen Finite-Elemente-Untersuchungen zielten auf die überlagerten Einflüsse des Schraubenabstände und der Biegesteifigkeit der Platte auf den Pressdruck ab. Des Weiteren wurde die Vorteilhaftigkeit einer versetzten bezüglich einer nicht versetzten Schraubenanordnung bei mehrreihiger Verschraubung untersucht.

Die Pressdruckvariation innerhalb der nominellen Einflussfläche einer Schraube nimmt extrem ausgeprägt mit dünneren, weniger biegesteifen Platten und mit zunehmenden Schraubenabständen zu. Die Berechnungsergebnisse stimmen mit punktbelasteten, elastisch gebetteten Balken und Platten qualitativ überein und wurden für eine große Bandbreite von Geometrie- und Steifigkeitskonfigurationen quantitativ erfasst.

Basierend auf den Berechnungsergebnissen wird ein neuer Pressdrucknachweis vorgeschlagen, der auf gemittelten Druckspannungen von Bereichen niedrigen Pressdrucks innerhalb der nominellen Druckeinflussfläche einer Schraube basiert. Die Widerstandsseite wird sodann, abweichend von ÖNORM B 1995-1-1 [14] als eine intrinsische Material- bzw. Klebstoffeigenschaft angesehen, die unabhängig von der jeweiligen geometrischen Konfiguration der Schraubenpressklebung ist. Innerhalb der untersuchten Grenzen von Plattensteifigkeit und Schraubenabständen ergaben versetzte Schraubenanordnungen kleinere lokal begrenzte Bereiche niedrigen Pressdrucks und sind somit bei mehrreihiger Schraubenanordnung, die bei größeren Rippenbreiten erforderlich ist, vorzuziehen.

1. INTRODUCTION

The concept of screw-gluing represents the application of the cramping pressure in wood bonding operations by means of self-tapping screws. In order to exert a pressure on the contact area and bond line between two adherends by means of screws, two major alternatives exist: In case of the widely prevailing method a partially threaded screw is used whereby the screw head and the unthreaded screw shaft are located in one of both adherends, in general being the thinner one and at the plate side of ribbed plates, whereas the threaded part of the screw is inserted into the opposite wooden component. The cramping pressure is then activated, once the screw head has full contact with the adjacent wood part and limited by the head pull-through capacity of the respective screw. Alternatively, fully threaded screws with varying thread inclination may be used [21].

Screw-gluing represents an advancement of its forerunner procedure, termed nail-press gluing, where the cramping force was applied by nails, formerly generally with unprofiled shaft. Screw-gluing is a highly versatile and cost-efficient possibility for applying bonding / cramping pressure to wooden adherends in face bonding operations which in general are performed by means of large hydraulic, pneumatic or vacuum presses. Screw-gluing is favorably used in cases where the bonding of the elements, the beams or parts of these cannot be performed by conventional presses or in cases where special and or very large cramping equipment is needed. So, frequent fields of applications of screw-gluing consist in the factory-based or in-situ applied reinforcement of notches and openings in glued laminated timber (GLT) beams by means of laterally bonded plywood or laminated veneer lumber (LVL) plates. An increasingly important field of screw-gluing is the manufacture of ribbed plates with single- or double-sided sheathing. Regarding material efficiency, ribbed plates are much more efficient than solid bulk timber plates, such as cross laminated timber (CLT) especially when a one-dimensional span situation is regarded, which is prevailing in praxis.

This paper addresses some basic screw-gluing aspects with a focus on its application to bonded ribbed plates. Hereby a few topics are addressed adding to a more comprehensive understanding and improved standardization of the regarded versatile jointing technology. Spacious reinforcements by means of screw-gluing e.g. for rehabilitation works of cracked shear areas of GLT beams and local reinforcements of openings and notches in beams are not regarded here explicitly.

The reported work represents a part of a larger effort in the frame of a substantial updating of the German timber design code DIN 1052-10 [12], which specifies several mainly bonding related additions to Eurocode 5 (EN 1995-1-1 [14]), and for the execution part of the presently drafted new Eurocode 5. The work is further related to research efforts in a "*Zukunft Bau*" research project on robotic assisted screw-gluing and supports novel construction solutions investigated in IntCDC, being one of Stuttgart University´s Clusters of Excellence.

2. STATE-OF-THE-ART IN SCREW-GLUING

At present screw-gluing is not addressed by any European product or design standard. Screw-gluing was normatively first addressed in the German standard DIN 1052-10 [12], specifying additional provisions for the design of timber structures. More recently the Austrian standard, ÖNORM B 1995-1-1 [13], providing national supplements for the implementation of EC5-1-1 [14] gives more detailed specifications on screw-gluing. Irrespective of the rather recent normative considerations of screw-gluing it is noteworthy that the precursor of this cramping methodology, then termed nail-gluing has been executed frequently from the very beginning of the last century in order to overcome the lack of sufficiently apt and large cramping equipment. So, a high number of the early GLT beams from 1910 to about 1940 are based on cramping pressure application by nail-gluing.

Earlier documented research work on specific aspects of nail-gluing, achievable cramping pressure levels and bond strengths were reported in Truax [10], Armbruster [1], Wassipaul [11], Brüninghoff [4] and Rabiej and Behm [7] (citation list not exhaustive). Later research on screw-gluing or other types of highly localized pressure applications were presented i.a. by Cheng and Sun [5], Stapf and Aicher [9], Bratulic and Augustin [3], Bratulic et al. [2], Franke et al. [6] and Rug et al. [8].

Following, the specifications provided by DIN 1052-10 and ÖNORM B 1995-1-1 are briefly presented as being the onset of the investigations and results discussed here.

2.1 SCREW-GLUING SPECIFICATIONS IN DIN 1052-10:2012 [12]

Screw-gluing acc. to [12] is reserved for bonding of solid wood boards and wood-based panels to other timber components. The panels may be plywood, oriented strand board (OSB), particle board or solid wood panels acc. to EN 13986 [17].

Laminated veneer lumber (LVL) acc. to EN 14374 [19] may be used when permitted by the respective technical data sheet or approval. The thickness of the boards and panel materials is limited to maximally 45 mm and 50 mm, respectively. The adherends onto which the boards and plates are bonded are unlimited with regard to size and may be structural solid wood, glued laminated timber (GLT), glued solid wood (GST), cross-laminated timber (CLT) or LVL.

Screw-gluing may be used for reinforcement of the cited adherend components, e.g. for reinforcement of GLT beams with holes and notches and, as regarded here, for manufacture of ribbed plates.

Adhesive issues, i.e. permissible adhesive families, required gap filling properties etc., specified in [12] and [13], are not addressed here as being rather irrelevant for the topics of this paper.

The provisions regarding screws and their arrangement are as follows:

i) The screws must be partially threaded and be of self-tapping type qualified by Technical application documents, i.e. conform either to the harmonized European standard EN 14592 [20] or to a European Technical assessment (ETA). The nominal diameter d of the screws must be ≥ 4 mm. In order to enable the exertion of a cramping pressure no screw thread shall be within the adhered board or plate. The thread length in the rib or any reinforced adherend must be minimally 40 mm or equal to the board / plate thickness, whichever is larger.

ii) Regarding the screw arrangement exclusively two requirements are stated. The nominal cramping pressure influence area of a single screw must not exceed 15,000 mm² and the spacing of the screws in any direction shall be ≤ 150 mm. No specifications are given e.g. for edge distances, what represents an obvious deficiency of the standard provisions.

In a brief summary of the screw-gluing provisions in [12] a striking necessity for an updating and amendment of the standard, presently on-going, is evident. It should be mentioned that in view of the outdated provisions in [12] a number of ribbed elements that go beyond the standard specifications have been constructed in Germany in recent years enabled by permissions of state (Länder) authorities based on expertises by MPA University Stuttgart.

2.2 SCREW-GLUING SPECIFICATIONS IN ÖNORM B 1995-1-1:2019

When compared to DIN 1052-10 the Austrian screw-gluing provisions published roughly a decade later are more elaborate. Hereby an attempt has been made to include later research, e.g. by Bratulic et al. [2] as well as grown industry experience. An effort has been made to differentiate between several size and material ranges and to provide further, so far missing construction detailing, e.g. on edge distances. However, several of the given provisions deserve a critical assessment and improvement.

In the following, apart from general rules, primarily the specifications in [13] addressing ribbed elements with CLT plates and GLT ribs are outlined. The thickness of the CLT plates can vary from 60 mm to 200 mm and hence ranges far beyond the current maximum plate thickness of 50 mm in [12]. Apart from more detailed provisions on spacings and edge distances, now for the first time requirements on the cramping pressure, exerted by the screws, and its respective calculation are given. In addition to tabulated screw spacings a calculation route for derivation of engineered / tailored spacings is specified, too.

Some of the mentioned add-ons are briefly outlined below. Fig. 1 shows the geometry notations, specified in [13] and adopted in this paper as well. The geometry notations address single and multiple screw row configurations of ribbed screw-glued timber plates. Notations on end distances, not relevant in this paper, are omitted in Fig. 1. In addition to [13] the length of the unthreaded shaft segment measured from the plate-rib interface to the start of the thread is now addressed by variable $l_{s,2}$. Note: Calculations performed in the context of this paper have shown that length $l_{s,2}$ presented in [13] merely as an undefined value ≥ 0 has a notable influence on the exerted interface pressure.

The calculation of the design cramping pressure per screw independent of a single or multiple screw arrangement and the pressure requirement is specified as (note: p_{cal} not given literally in [13])

$$p_{cal,d} = F_{ax,d}/(a_1 \cdot a_2) \geq p_{cal,min} \quad (1)$$

where

$F_{ax,d} = F_{ax,k} \cdot \frac{k_{mod}}{\gamma_m}$ design screw head pull-through capacity

$F_{ax,k} = f_{head,k} \cdot d^2$ characteristic screw head pull-through capacity

$$f_{head,k} = 14 \cdot {d_h}^{-0.14} \cdot \left({\rho_k}/{\rho_{ref,k}}\right)^{0.8} \quad (2)$$

screw head pull-through parameter for softwood

$f_{head,k} = 25\ N/mm^2$ screw head pull thr. param. for beech LVL plates

$k_{mod} = 1.0$ and $\gamma_m = 1.3$ and $\rho_{ref,k} = 350\ kg/m^3$

$p_{cal,min}$ required minimum pressure

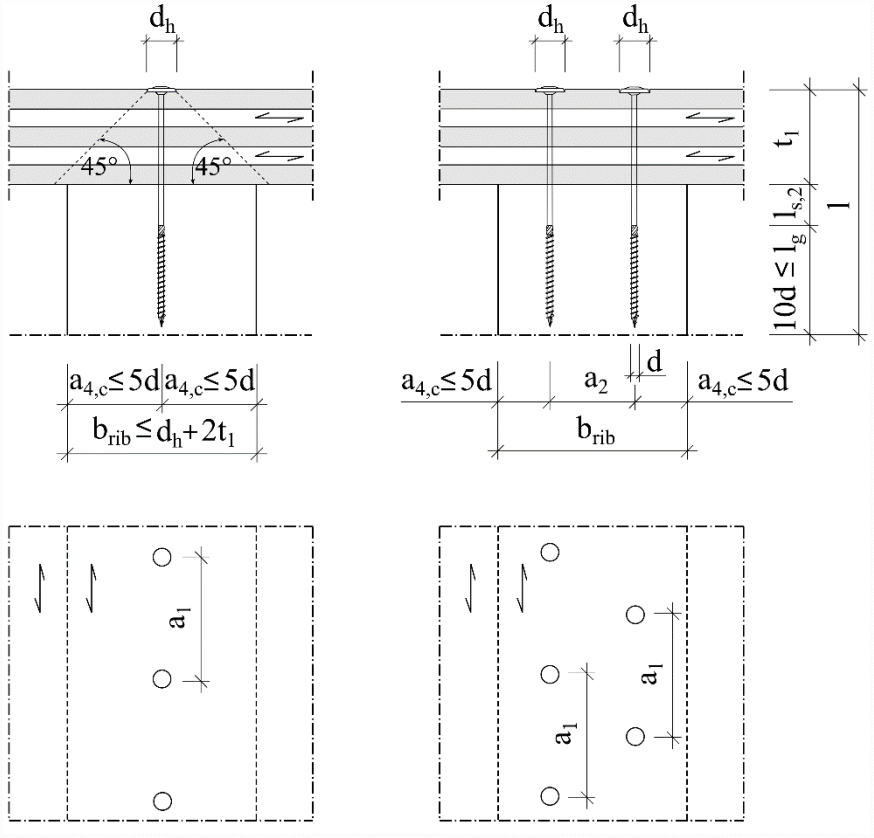

Fig. 1: Geometry notations for spacings and edge distances of screw-glued ribbed timber plates acc. to ÖNORM B 1995-1-1 [13]

Not going too much into details and some critics, the following should be stated. In principal the k_{mod} and γ_m factors are meaningless in the present short-term application context for obvious reasons and were assumingly maintained to enable a formal sticking to the conversion of characteristic to design values. The specified k_{mod} and γ_m numbers address acc. to [13] in cumulative manner the pressure relaxation during the cramping time.

Equation (2) for the characteristic head pull-through parameter can be disputed as the $f_{head,\,k}$ values are part of all relevant ETAs and respective DOPs of the screw manufacturers. However, Eq. (1) for the calculated design cramping pressure per

screw is apparently wrong. For a single screw row configuration (Fig. 1) dimension a_2 is irrelevant and for multiple screw row configurations the equation delivers wrong nominal pressure results. For correct equations see chapter 5. The values for the required minimum cramping pressure are specified in Table 1, here given as an excerpt of the full table NA.L.9 in [13].

Table 1: Screw-gluing specifications for ribbed timber CLT-GLT plates acc. to [13] including screw dimensions, spacings and cramping pressure requirements

Material of the plate	thickness of the plate	screw diameter	head / washer diameter	max. screw distances		thread length in the rib	nominal min. cramping pressure
				parallel to fiber	orthogonal to fiber		
	t_1*	d	d_h	$a_{1,max}$	$a_{2,max}$	l_g	$p_{cal,min}$
	[mm]	[mm]	[mm]	[mm]	[mm]	[mm]	[N/mm²]
CLT and GLT	$60 \le t_1 \le 100$	≥ 8	30	225	160	10·d	0.18
	$100 \le t_1 \le 200$		45	250	200	15·d	0.25

*) note: t_{cl} changed to t_1

The specified cramping pressure requirements vary significantly depending on plate thickness. The required pressure ranges from 0.10 N/mm² for plywood and solid wood boards with thicknesses of 12 to 18 mm (not shown here) up to 0.25 N/mm² in case of ribbed elements with CLT plates with thicknesses of 100 mm to 200 mm. The plausibility of the cramping pressure increase for thicker plates all together with the absolute stress levels and further the calculation of the applied pressure based on an apparent mean stress in the interface is subject of some considerations in this contribution. Besides the cramping pressure requirements Table NA.L.9 in [13] and the respective truncated Table 1 specify maximum spacings $a_{1,max}$ and $a_{2,max}$ parallel and perpendicular to the wood fiber direction of the (deck-) plate assumed to coincide with the longitudinal axis of the rib.

The tabulated recommended screw diameters d, the minimum values for the screw head-/washer diameters d_h (note: a ratio of $d_h/d \ge 1.8$ is prescribed) and the minimum anchorage lengths l_g of the threaded screw part in the substrate, here the rib, as well as the values of most other parameters are differentiated with regard to thickness of the (deck-)plate and the plate materials. While spacings $a_{1,max}$ vary in

a rather perceivable range, the distances $a_{2,max}$ are considered being too high in case of several configurations, yet not followed up here.

In addition to the tabulated maximum values for the spacings, these can be calculated individually, too, as

$$a_{i,max} = 3.35 \cdot \sqrt[4]{E_{mean,i} \cdot I_{i,b=1}} \quad (3a)$$

where

$I_{i,b=1}$ moment of inertia [mm^4] in i-direction

$E_{mean,i}$ mean MOE [N/mm²] in i-direction.

In case of homogenous isotropic or orthotropic board or plate materials, e.g. particle boards or plywood, with a nominally constant (smeared) MOE within total plate thickness t_1 or in case of layered buildups (CLT) with an apparent substitute MOE, Eq. (3a) can be rewritten as

$$a_{i,max} = 1.8 \cdot \sqrt[4]{E_{mean,i} \cdot t_1^3} \,. \quad (3b)$$

Equations (3a, b) result from calculations for beams on elastic foundation, being in principle a plausible mechanical approach. However, in most cases the Eqs. (3a, b) deliver entirely unrealistic $a_{i,max}$ values which then have to be reduced by the limiting mean cramping pressure verification (Eq. (1)). The custom-tailored approach by Eqs. (3a, b) deserves deepened consideration and is not considered appropriate in its present form for a standard.

3. INVESTIGATED SCREW-GLUING ASPECTS AND CONFIGURATIONS

The reported numerical investigations aimed at two important basic features of screw-gluing of ribbed timber plates, being

i) the superimposed effect of screw spacing a_1 parallel to the rib length axis and of the bending stiffness of the deck plate (simulation series A). The investigated screw spacings a_1 range from 125 to 300 mm. The thicknesses and the strong axis bending stiffnesses of the CLT deck plates range from 60 mm to 200 mm and (190 to 5800)·10³ kNmm² for the strong direction 1, parallel to the rib axis. All calculations were performed with a constant GLT rib width of 100 mm.

ii) a comparison of not staggered and staggered screw placement of screws inserted in two parallel rows (simulation series B). At the staggered and not staggered arrangement two screw spacings of 150 mm and 200 mm were considered. The calculations on the screw placement issues were performed with a 3-layered CLT plate (t_1 = 60 mm) and a rib width $b_{rib=}$ 120 mm).

In all cases the plates of the ribbed elements consisted of cross laminated timber (CLT) of either three or five layers with layer thicknesses of either 20 mm (plate thickness t_1 = 60 mm and 100 mm) or 40 mm (t_1 = 200 mm). The strength class of the CLT boards was C24 acc. to EN 338 [16]. The ribs were assumed to be made from homogenous GLT, strength class GL24 acc. to EN 14080 [18]. The screws with washer-type heads were partially threaded and had a constant nominal diameter of d = 8 mm. The head diameter was in all cases d_h = 22 mm. The lengths of the screws varied according to the thickness of the CLT deck plate and are specified below in detail.

Tables 2 and 3 contain the geometric details of all analyzed configurations.

Table 2: Compilation of geometry configurations of simulation series B of screw-glued CLT-GLT rib plates

configuration	plate thickness; (layer thickness) [GLT rib width]	screw spacings			staggered by $a_1/2$	screw dimensions d (l) $[l_{thread}]$ $\{d_h\}$	$f_{head,k}$
		a_1	$a_{4,c}$	a_2			
	[mm]	[mm]	[mm]	[mm]		[mm]	[N/mm²]
B_150_n	60 mm (3 x 20 mm) [120 mm]	150	30	60	no	8 (160) [80] {22}	10
B_200_n		200					
B_150_s		150	(3.75·d)	(7.5·d)	yes		
B_200_s		200					

Table 3: Compilation of geometry configurations of simulation series A of screw-glued CLT-GLT rib plates

configuration	plate thickness t_1; (layer thickness) [GLT rib width]	moments of inertia I_1 [$I_{2]}$]	screw spacing a_1	screw dimensions d (l) [l_{thread}] {d_h}	$a_{x,max}$ ($a_{y,max}$)
	[mm]	[mm^4]	[mm]	[mm]	
A_60_125	60 mm (3 x 20 mm) [100 mm]	17.330 [667]	125	8 (220) [100] {22}	394 (174)
A_60_150			150		
A_60_175			175		
A_60_200			200		
A_60_225			225		
A_60_250			250		
A_60_300			300		
A_100_125	100 mm (5 x 20 mm) [100 mm]	66,000 [17.330]	125	8 (260) [100] {22}	550 (394)
A_100_150			150		
A_100_175			175		
A_100_200			200		
A_100_225			225		
A_100_250			250		
A_100_300			300		
A_200_125	200 mm (5 x 40 mm) [100 mm]	528,000 [138.667]	125	8 (320) [100] {22}	925 (662)
A_200_150			150		
A_200_175			175		
A_200_200			200		
A_200_225			225		
A_200_250			250		
A_200_300			300		

4. MODELLING DETAILS

The 3D Finite Element calculations were performed with the commercial software ANSYS (version 19.2) using 4-node tetrahedrons (element type SOLID186). The rib was meshed as one orthotropic continuum whereas the CLT plate was modelled with discrete solid wood board layers arranged orthogonally to each other. The stiffness numbers assumed in the calculations for the CLT boards and the GLT rib of strength classes C24 and GL24, respectively, are given in Table 4. The screws were modelled in discrete approximative manner whereby the periphery of the unthreaded screw shaft of diameter d fits contactless into a hole of same diameter in the CLT and GLT. The threaded screw part was not modelled in true geometry but with a smooth cylinder surface, then connected rigidly to the surrounding GLT timber. The washer-type screw head influencing the pressure distribution significantly was discretized with true dimensions. First calculations showed that the length of the unthreaded shaft segment in the GLT substrate, $l_{s,2}$, has mechanically plausible a noticeable influence on the interface pressure distribution. So, $l_{s,2}$ was throughout taken as 60 mm, i.e. 7.5 times of the nominal screw diameter d = 8 mm. Details of the $l_{s,2}$ influence are not discussed in this paper.

Calculations performed with solid to solid contact in the interface as well as with rigidly connected surfaces / nodes, did not reveal substantial differences for the interface compressive stresses in case of the regarded rather thick plates. Hence in the reported parameter study for reason of saving on computation time a rigid CLT-GLT connection was assumed. For thinner, less stiff plates, not regarded here, a contact modelling is necessary; the respective differences are revealed in a separate contribution.

Table 4: Constitutive properties of CLT boards and GLT rib assumed in the analysis

	E_1 [N/mm²]	$E_{2,3}$ [N/mm²]	$G_{12} = G_{13}$ [N/mm²]	G_{23} [N/mm²]	$\nu_{12} = \nu_{13}$ [-]	ν_{23} [-]
CLT boards (C24)	11.000	370	690	69	0.015	0.35
GLT rib (GL24c)		300*	650	65		

*) results given here apply to $E_{2,3}$ = 370 N/mm²

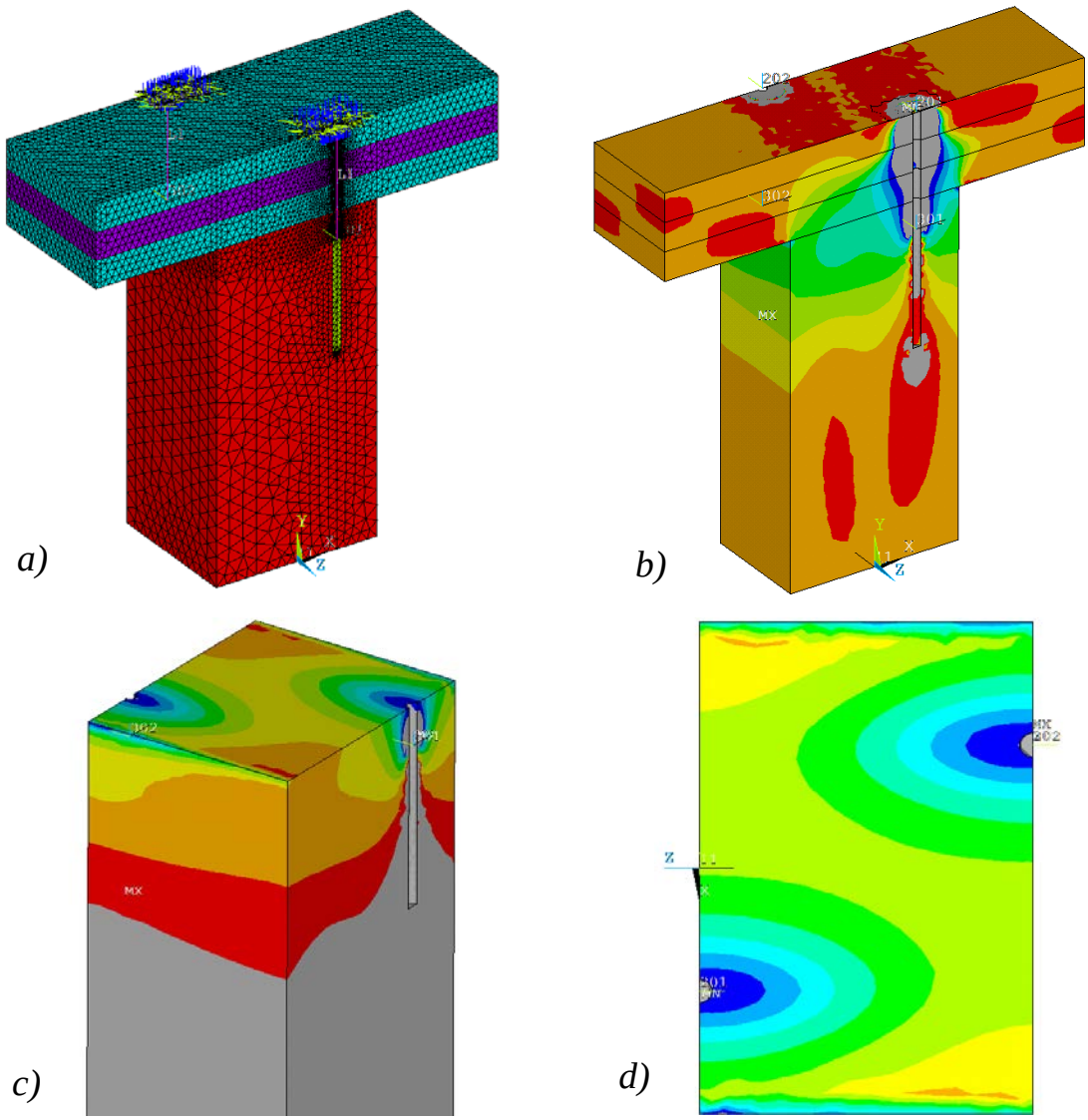

Fig. 2: Finite element calculations on the compressive stresses exerted by screws in the plate-rib interface of screw-glued ribbed CLT-GLT elements
a) discretized FE-model representing a staggered two-row screw arrangement
b) compressive stresses $\sigma_{c,90}$ normal to plate and interface plane in the CLT plate and the GLT beam
c), d) $\sigma_{c,90}$ in the interface and (exclusively c)) in GLT

The pressure activation by the screw was realized by generating a thermal contraction of the unthreaded screw shaft until iteratively the head pull-through capacity of the specifically employed screw is reached, as done e.g. by Bratulic [2].

The symmetry conditions of the investigated configurations were considered. So, in case of a single screw row at mid-width exclusively a CLT-GLT segment of length $a_1/2$ and width $b_{rib}/2$ was analyzed. In case of two screw rows arranged in parallel, the model dimensions were $a_1/2$ in beam length direction and orthogonally hereto the full rib width. Hereby the centers of both screws are hit at $\xi=0$

(not staggered arrangement) or at ξ=0 and ξ=0.5 in case of the staggered arrangement, see Figs. 9 and 10. The CLT plate overhang perpendicular to the rib axis was throughout taken as 80 mm. Fig. 2a visualizes the model discretization of the ribbed element for the case of a thin (60 mm) 3-layered CLT plate and a staggered screw arrangement. Fig. 2b shows the compressive stress distribution exerted by the screws at the upper CLT surface and within a vertical section including the intersecting screws. Fig. 2c reveals for the regarded build-up the compressive stress distribution in the CLT-GLT interface and in the GLT. Finally, Fig. 2d shows the compressive stress isolines in a top view of the interface plane.

5. SIMULATION RESULTS

The cramping pressure distributions presented below are given throughout in normalized manner in order to enable a better comparison of the different configurations. The mean nominal pressure p_{nom} exerted by the head pull-through capacity of the screw is calculated with the nominal influence area of the screw, being

$$A_{cramp,nom} = a_1 \cdot b_{rib} \quad \text{(single row screw appl.)} \quad (4)$$

$$A_{cramp,nom} = a_1 \cdot (a_{4,c} + a_2/2) = a_1 \cdot b_{rib}/2 \quad \text{(double row screw appl.)} \quad (5)$$

The normalization of the local pressure $p_{cramp,loc}$ is then obtained from the ratio $p_{cramp,loc}/p_{nom}$, being equal as applying $p_{nom} = 1.0\ N/mm^2$. The distance along the spacing a_1 between successive screws and the location within edge distance $a_{4,c}$ or the distance a_2 between screws perpendicular to rib width are given normalized as ξ and η, too. Preceding a closer quantitative discussion of the results, Fig. 3 illustrates in coarse qualitative manner the spacious cramping pressure distributions (isolines) normal to the plate-rib interface of simulation series A and B, where configuration dependent significant differences can be seen.

5.1 RESULTS OF SERIES A

For each of the regarded built-up configurations specified in Table 3 the pressure distributions are given for three selected paths 1 to 3, shown in Fig. 3a. Hereby path 1, stretching parallel to the rib length axis is located at mid-width of the rib (y = η= 0) and starts at the screw location x = ξ = 0. Paths 2 and 3 stretch perpendicular to the rib axis starting at x = ξ = 0 and ξ = 2x / a_1, respectively (see Fig. 3a). Figs. 4, 5 and 6 reveal the cramping pressure results for the three investigated

very different plate stiffness configurations, depending in all cases parametrically on the screw distance a_1.

It is immediately evident that the unconformity of the pressure distribution increases with larger screw spacing a_1 as well as with reducing bending stiffness and thickness of the plate. Mechanically utmost plausible, the highest pressure in the rib-plate interface occurs immediately at the screw location, shown in Figs. 4b, 5b and 6b. This feature is highly pronounced in case of the thin plate (t = 60 mm) with low bending stiffness $(EI)_1 = 190 \cdot 10^3$ kNmm² and much less articulate at the thick plate (t = 200 mm) with a 30 times higher bending stiffness.

Similarly plausible, the lowest cramping pressure occurs at mid-length between the screws, $\xi = 2x / a_1 \approx 0.5$, and hereby close to the edges of the rib width $b = b_{rib}$. The minimum pressure values actually are not located directly at the very edges at ± b/2, but close to these at $0.4 \lesssim \eta = 2y/b \lesssim 0.45$. Within the η-range of 0.45 to 0.5, at the outermost 10% of the rib width a significant stress increase towards the edges at ± b/2 occurs. This local contact pressure rise increases with growing plate stiffness, and is most pronounced at the thick plate (Figs. 6c and d). The stress increases result from the geometric discontinuity at the plate – rib intersection and are best envisioned when the rib is conceived as a concentrated punching force acting on a more or less stiff foundation.

For a more accurate assessment of the pressure variation within the cramping area, the most relevant quantitative numbers of the pressure distribution being

i) the maximum value p_{max} at the screw location ($\xi = \eta = 0$),

ii) the minimum value $p_{min} = p_{3,min}$ at $\xi = 0.5$ and $0.4 \lesssim \eta \lesssim 0.5$ and

iii) ,iv) $p_{2,min}$ and $p_{3,0}$ at two further prominent positions of paths 2 and 3

are summarized in Table 5. In addition, the table specifies as a single indicator of the pressure unconformity the pressure ratio $r_{p,\Delta} = \frac{p_{min}}{p_{max}}$.

Fig. 7 shows a graphical representation of the cramping pressure ratio $r_{p,\Delta}$ depending on the spacing variable a_1 and on the plate bending stiffness $(EI)_1$ in rib-length direction. The $r_{p,\Delta}$-curves reveal that the spacing effect increases markedly with reduced plate stiffness.

Finally, in order to capture and quantitatively describe the bonding relevant minimum pressures within the influence area of a screw the two-dimensional relationship $p_{min} = f(a_1, (EI)_1)$ is shown in Fig. 8. Given are the discrete values of Table 5 and a continuous approximation surface derived by least square minimization specified quantitatively in Eq. (7) in chapter 6.

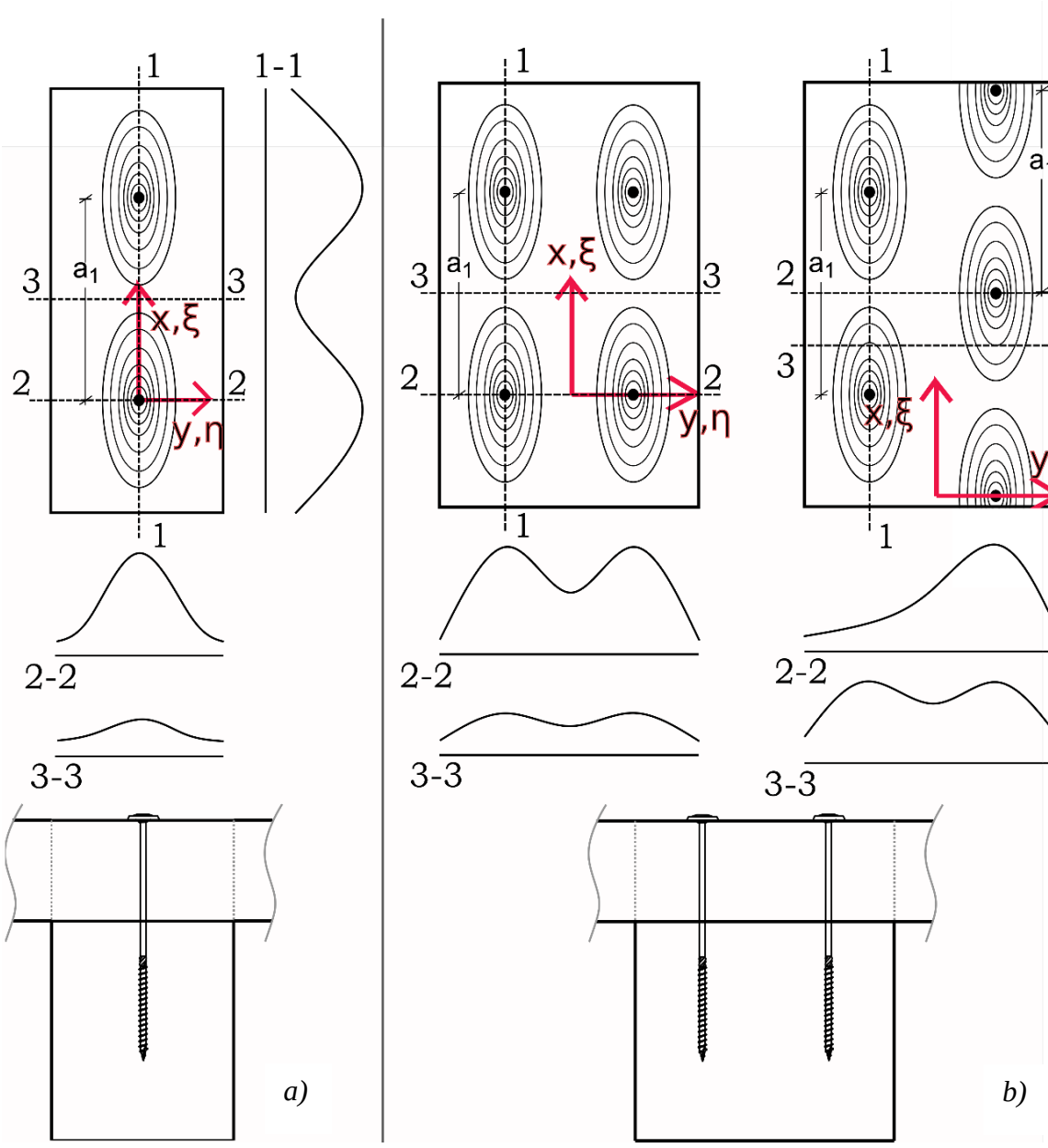

Fig. 3: Location of paths 1-3 and cramping pressure sketch of isolines of investigated screw-glued rib plate configurations.
a) simulation series A *b) simulation series B*

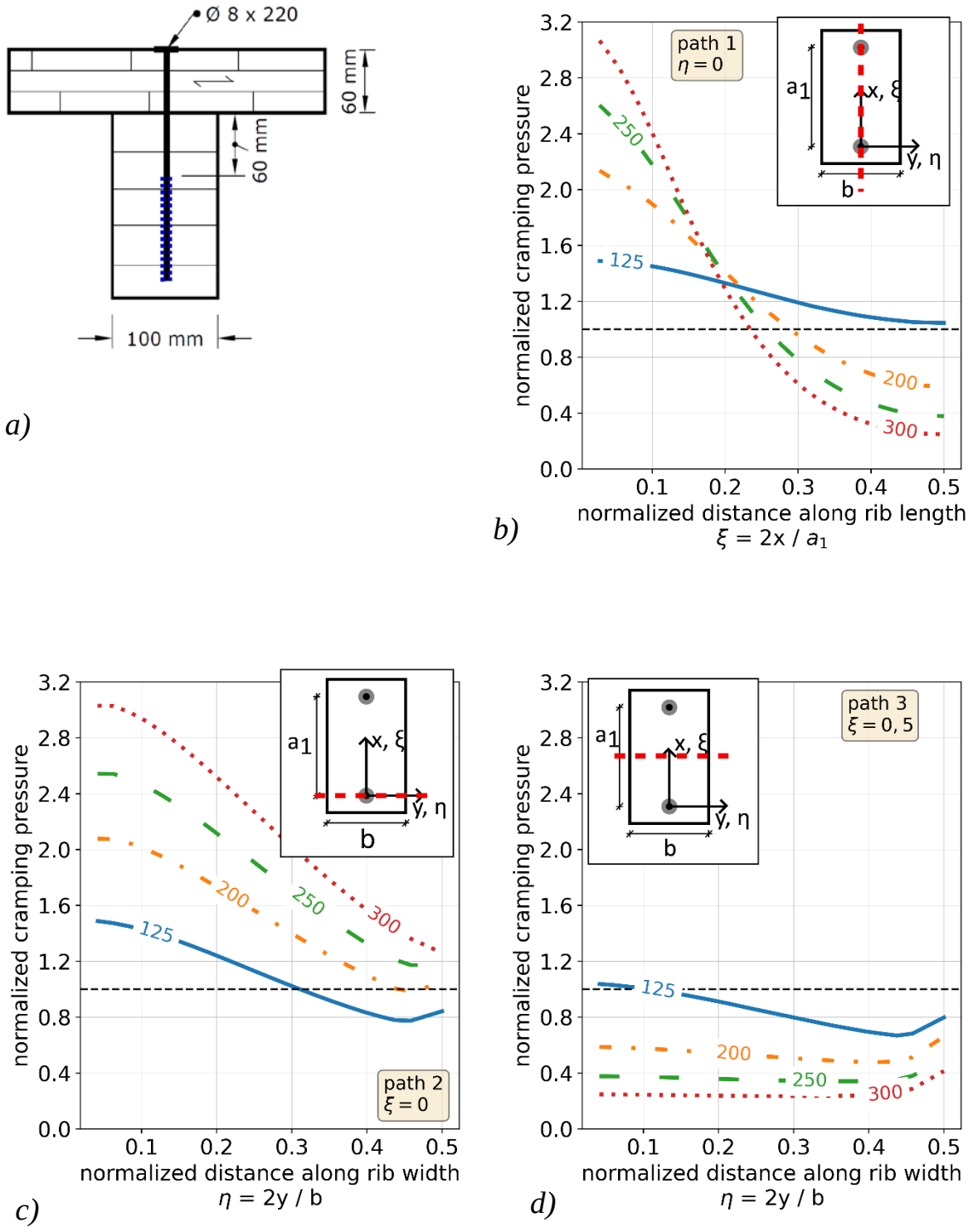

Fig. 4: Cramping pressure p_{cramp} results (normalized to mean pressure) in the plate-rib interface for a thin CLT plate (60 mm) depending on screw spacing in single row arrangement (simulation series A)
a) analysed cross-sectional geometry and dimensions
b) p_{cramp} at mid-width of rib along path 1 parallel to rib axis
c) p_{cramp} along path 2 perpendicular to rib axis at $\xi = 0$
d) p_{cramp} along path 3 perpendicular to rib axis at $\xi = 0.5$

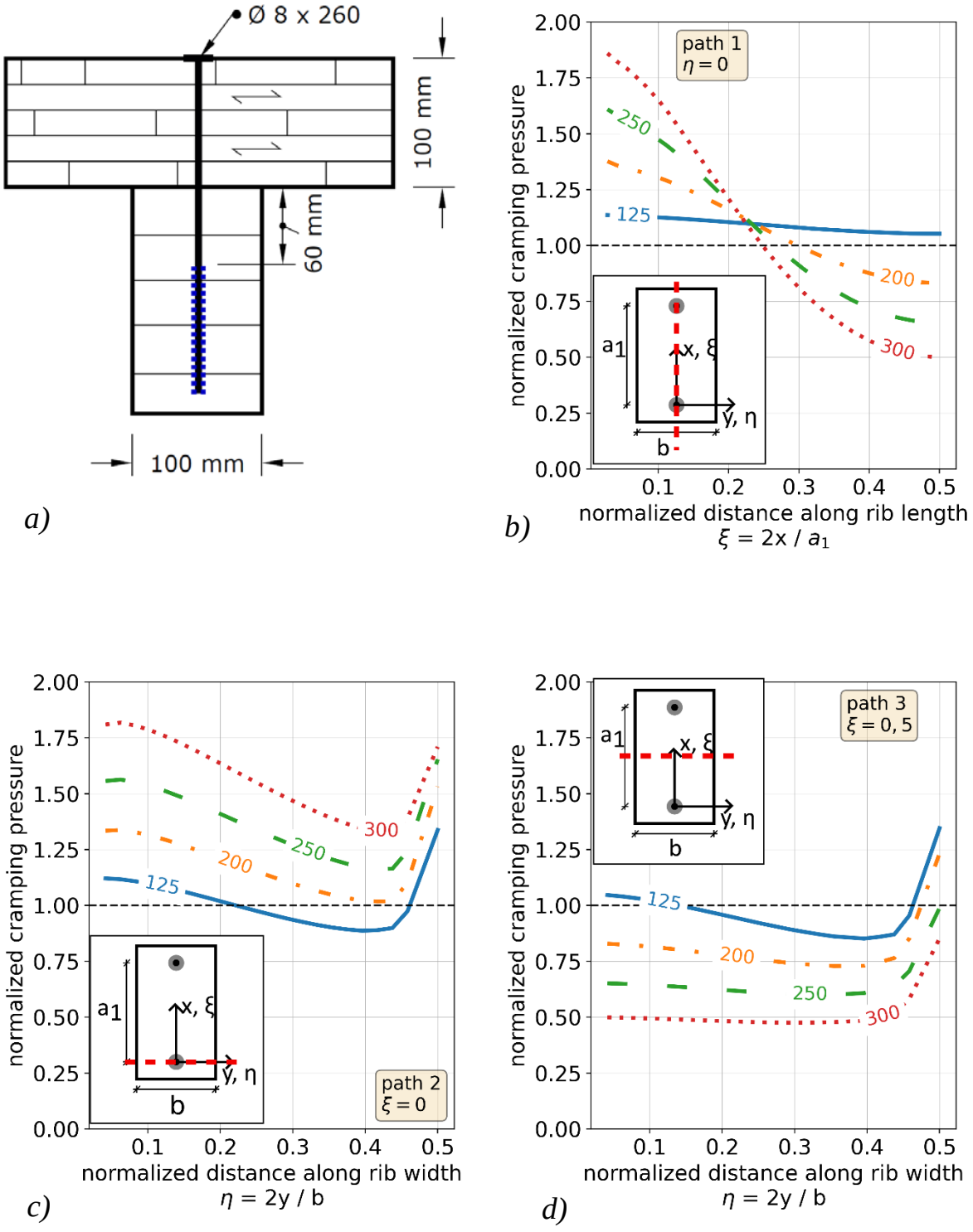

Fig. 5: Cramping pressure p_{cramp} results (normalized to mean pressure) in the plate-rib interface for a medium thick CLT plate (100 mm) depending on screw spacing in single row arrangement (simulation series A)
a) analysed cross-sectional geometry and dimensions
b) p_{cramp} at mid-width of rib along path 1 parallel to rib axis
c) p_{cramp} along path 2 perpendicular to rib axis at $\xi = 0$
d) p_{cramp} along path 3 perpendicular to rib axis at $\xi = 0.5$

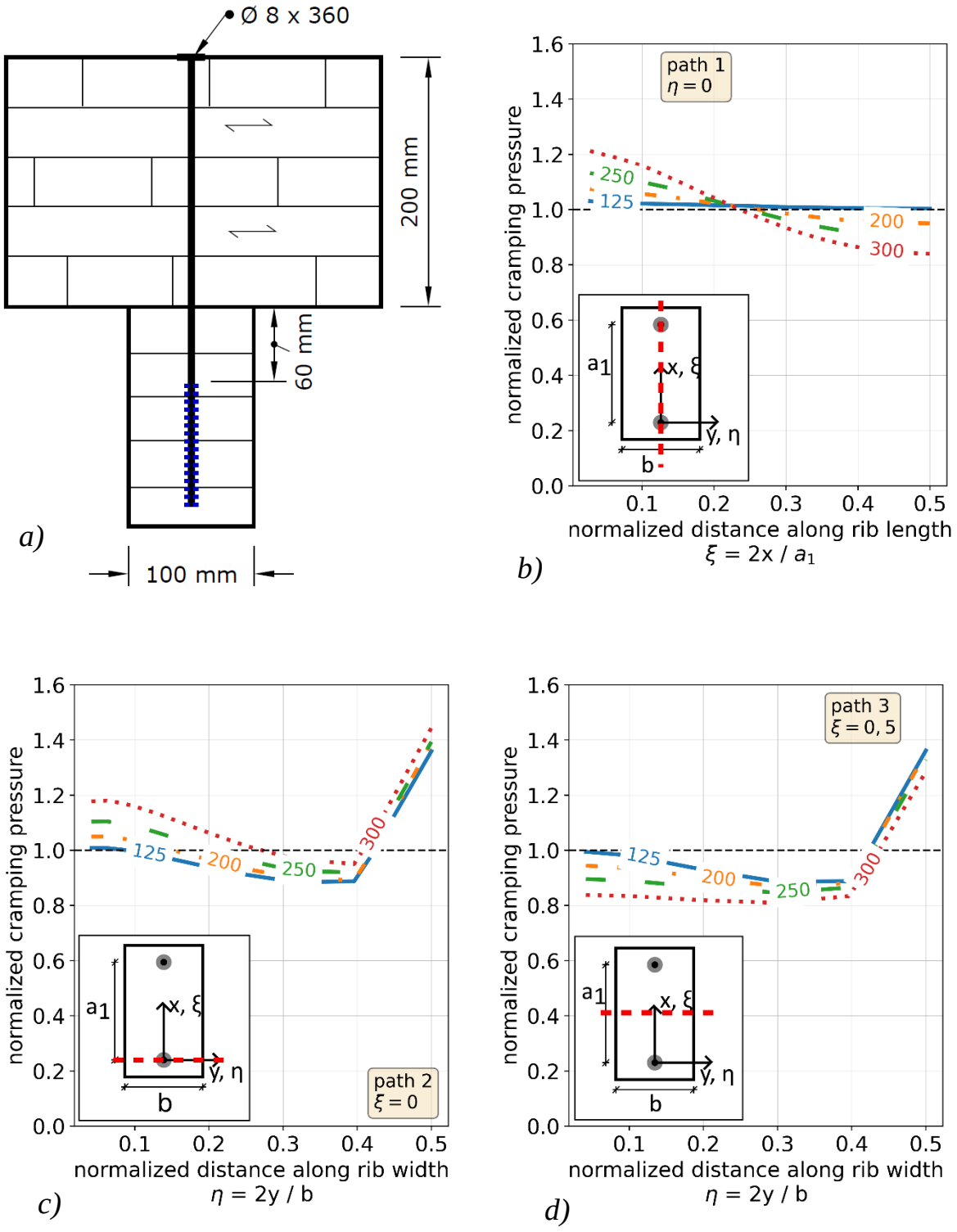

Fig. 6: Cramping pressure p_{cramp} results (normalized to mean pressure) in the plate-rib interface for a thick CLT plate (200 mm) depending on screw spacing in single row arrangement (simulation series A)

a) analysed cross-sectional geometry and dimensions

b) p_{cramp} at mid-width of rib along path 1 parallel to rib axis

c) p_{cramp} along path 2 perpendicular to rib axis at $\xi = 0$

d) p_{cramp} along path 3 perpendicular to rib axis at $\xi = 0.5$

Table 5: Normalized cramping pressure values at specific locations and extreme value ratios of all screw-gluing configurations of simulation series A

Configu-ration	Normalized cramping pressure (location)				
	p_{max} ($\xi = \eta = 0$)	$p_{2,min}$ ($0.4 \lesssim \eta \lesssim 0.5$)	$p_{3,0}$ ($\eta = 0$)	$r_{p,min} = p_{min} = p_{3,min}$ ($0.4 \lesssim \eta \lesssim 0.45$)	$r_{p,\Delta} = \frac{p_{min}}{p_{max}}$
60_125	1.49	0.77	1.05	0.67	0.45
60_150	1.69	0.84	0.89	0.62	0.37
60_175	1.91	0.91	0.73	0.55	0.29
60_200	2.18	0.98	0.59	0.48	0.22
60_250	2.67	1.17	0.38	0.34	0.13
60_300	3.17	1.26	0.25	0.23	0.07
100_125	1.14	0.89	1.05	0.85	0.75
100_150	1.19	0.91	1.0	0.83	0.7
100_175	1.28	0.96	0.92	0.78	0.61
100_200	1.4	1.02	0.83	0.73	0.52
100_250	1.64	1.16	0.65	0.6	0.37
100_300	1.91	1.33	0.5	0.47	0.25
200_125	1.03	0.89	1.0	0.89	0.86
200_150	1.04	0.89	0.99	0.88	0.85
200_175	1.05	0.89	0.97	0.88	0.84
200_200	1.09	0.89	0.95	0.87	0.8
200_250	1.15	0.92	0.90	0.85	0.74
200_300	1.23	0.95	0.84	0.81	0.66

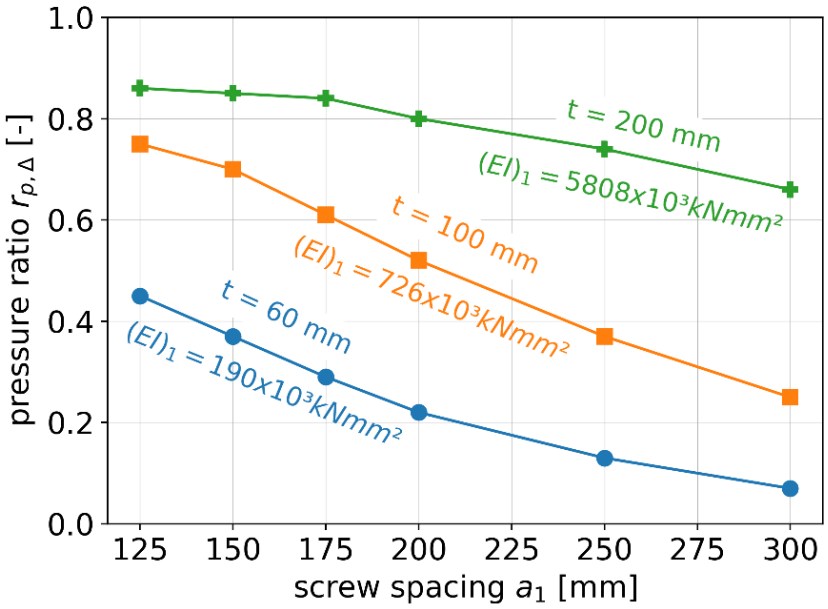

Fig. 7: Pressure ratios $r_{p,\Delta}$ of investigated screw-gluing configurations of simulation series A

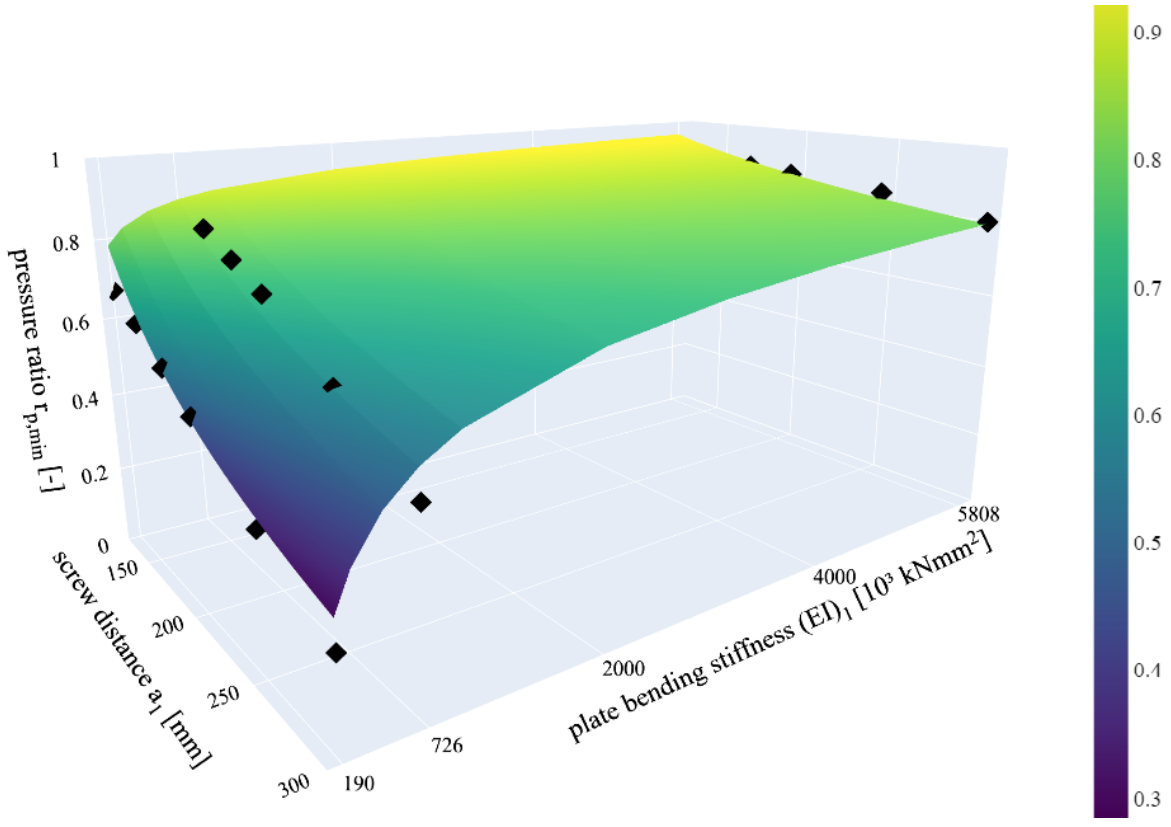

Fig. 8: Minimum pressure ratio $r_{p,min}$ values and fit surface (see chap. 6, Eq. (7)) depending on variables a_1 and $(EI)_1$ resulting from simulation series A

5.2 RESULTS OF SERIES B

Figs. 9 and 10 reveal the cramping pressure results for the not staggered and staggered screw arrangements investigated in simulation series B with two spacings a_1 of 150 mm and 200 mm. For both screw arrangements the contact area pressure distribution is given for path 1 along the rib axis stretching between two consecutive screws. Further, the stress distribution is shown for two paths, 2 and 3, perpendicular to the beam axis. Path 2 is located at $\xi = 0$ and intersects with one or both screws depending on the respective configuration, being staggered or not staggered. Path 3 is located between the screws along beam length axis at $\xi = 0.5$ and $\xi = 0.25$ in case of the not staggered and staggered arrangements, respectively.

Path 1: The pressure distribution is, as anticipated, very similar for both configurations yet not identic, see Figs. 9b and 10b. Further, the stress distributions resemble qualitatively the stress curves given in Fig. 3 for the single screw row arrangement investigated with a rather similar slab-rib configuration (note the different rib widths of 100 mm and 120 mm). Quantitatively the pressure curves in Figs. 9 and 10 can be compared for a_1 = 200 mm.

Significant differences between the staggered and not staggered configuration can be seen in case of the stress distributions along paths 2 and 3 perpendicular to the beam axis.

Path 2, not staggered screw configuration:

The stress distribution is symmetric to beam mid-width $\eta = 0$ with two stress peaks at the screw locations (Fig. 9c). Hereby it is interesting to note that the stresses between both screws, spaced at a distance $a_2 = 2 \cdot a_{4,c}$, decrease lesser than in the outer ranges $a_{4,c}$ between the screw and the beam edges at $\pm\, b\,/\,2$. The fact, that the stress level between the screws is higher although the nominal influence lengths towards the edges at $\pm b/2$ and in between the two screws are chosen equal as $a_{4,c} = a_2/2$ shows a mutual influence of the neighboring screws. This can be anticipated however the quantitative differences of the minimum stress levels within $a_{4,c}$ and a_2, being strongly influenced by the plate stiffness perpendicular to beam axis and distance a_2 is subject to calculations not shown here. It is strongly doubted that the very large distances a_2 specified in [13] and Table 1, with upper limits of a_2 = 160 mm and 200 mm for plate thicknesses from 60 up to 99 mm and from 100 up to 200 mm, respectively,

ensure for the inter-screw distance a_2 a stress level equal or higher to that in the edge distance regions $a_{4,c}$.

Path 2, staggered screw configuration:

The pressure distribution along path 2 is in this case highly asymmetric with respect to the beam mid-width as shown in Fig. 10c. While the stress decline from the screw to the closer adjacent beam edge at $\eta = + 0.5$ conforms almost exactly to the curves given for the not staggered build-up, a pronounced stress reduction occurs in the range of $-0.5 < \eta < 0$. For a quantitative comparison of the different screw arrangements beyond local minimum value (see below) averaged stress values are calculated for the width range of $-0.5 \lesssim \eta \lesssim -0.25$. These are 0.52 and 0.69 in case of a_1 = 200 mm and 150mm, respectively.

Path 3: The stress distributions along this path are shown in Figs. 9d and 10d. In case of the not staggered build-up this section marks the lowest stress level which is almost constant along the rib width for a_1 = 200 mm and just slightly fluctuating in case of a_1 = 150 mm. Note: The stress peaks at ± b/2 discussed above are disregarded. In the graphs the mean stress levels (outer peak ranges excluded) are given, too. These are 0.45 and 0.68 in case of a_1 = 200 mm and 150 mm, respectively, for the not staggered build-up. The stress distributions resemble those given in Fig. 4d well. In case of the staggered configuration, the stress distribution along path 3 is plausibly symmetric with respect to the beam mid-width. Further, the mean pressure level is much higher as compared to the not staggered arrangement and shows a larger variation resembling shape-wise the not staggered configuration well.

The comparison of the staggered and not staggered screw configurations is performed on the basis of the smeared minimum stress levels. In detail, the above stated averaged minimum stress levels of the not staggered configuration along path 3 (Fig. 9d) are compared with the locally averaged mean minimum values of the staggered build-up (Fig. 10c). The comparison is graphically depicted in Fig. 11a and b. It can be seen that the minimum mean cramping pressures of both screw arrangements are very close to each other in case of a_1 = 150 mm. At a_1 = 200 mm the stress level of the staggered arrangement (0.52) exceeds the level of the not staggered configuration (0.45) roughly by 10%. Based on the fact that the spatial extension of the compared minimum mean stress levels is much larger in case of the not staggered screw placement, the staggered arrangement is calcula-

tion-wise much preferable. This conclusion is based on the considered cross-sectional build-up configurations and is certainly valid well beyond. However, deepened parametric studies are necessary in order to generalize the above findings to a much wider range of cross-sections and screw placement configurations.

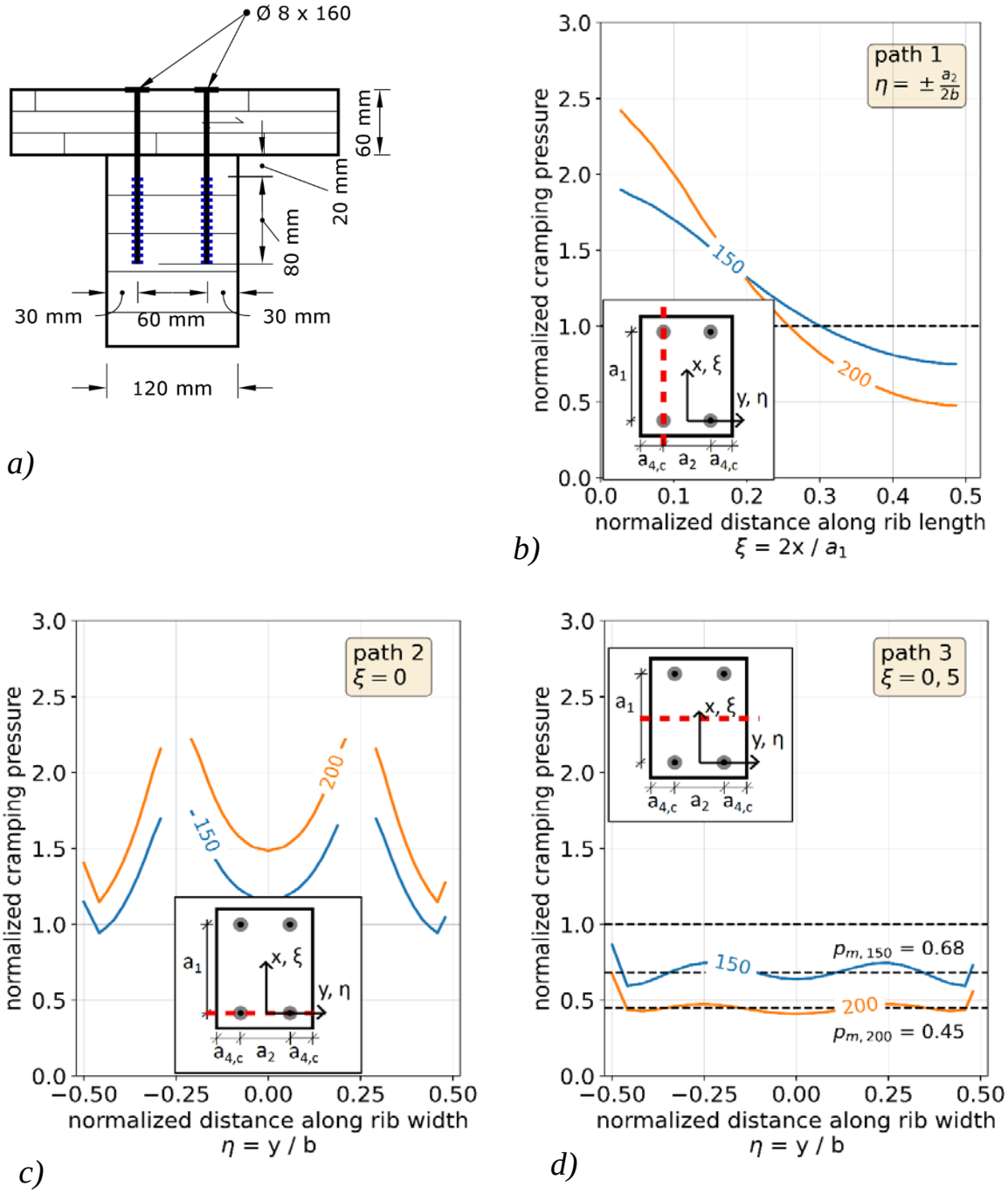

Fig. 9: Cramping pressure p_{cramp} results (normalized to mean pressure) in plate-rib interface for parallel (2-row), not staggered arrangement (simulation series B)
a) analysed cross-sectional geometry and dimensions,
b) p_{cramp} along path 1 parallel to rib axis ($\eta = \pm a_2/2b$),
c) p_{cramp} along path 3 perpendicular to rib axis at $\xi = 0$,
d) p_{cramp} along path 3 perp. to rib axis at half distance between screws ($\xi = 0.5$)

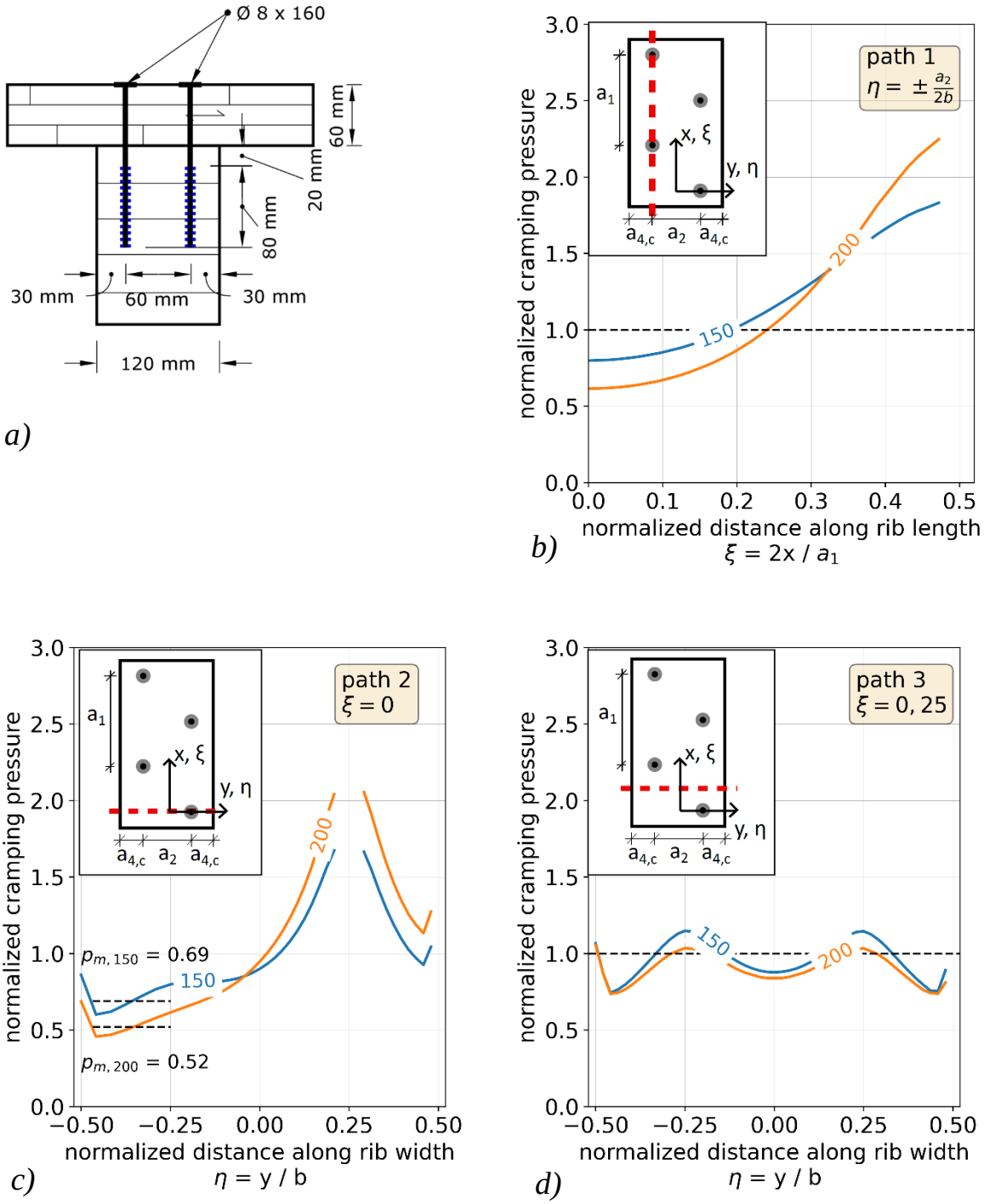

Fig. 10: Cramping pressure p_{cramp} results (normalized to mean pressure) in plate-rib interface for parallel (2-row), staggered arrangement (simulation series B)
a) analysed cross-sectional geometry and dimensions,
b) p_{cramp} along path 1 parallel to rib axis ($\eta = \pm a_2/2b$),
c) p_{cramp} along path 3 perpendicular to rib axis at $\xi = 0$,
d) p_{cramp} along path 3 perp. to rib axis at half distance between two staggered screws ($\xi = 0.25$)

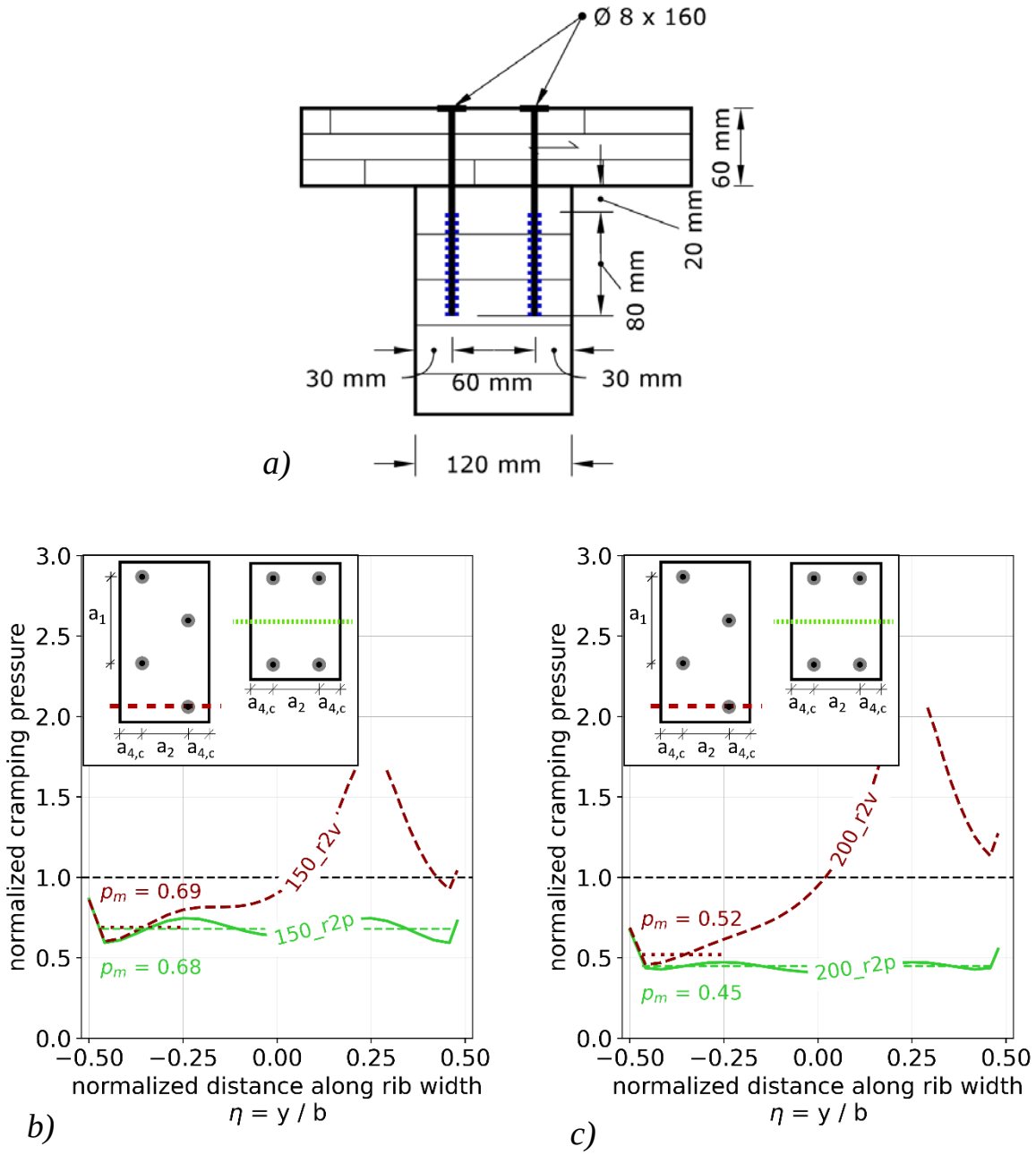

Fig. 11: Result comparison of simulation series B with not staggered and staggered screw arrangement for the paths with the lowest cramping pressure
a) analysed cross-sectional geometry and dimensions
b) screw spacing in rib-length direction a_1 = 150 mm
c) screw spacing in rib-length direction a_1 = 200 mm

6. DISCUSSION

The pronounced cramping pressure variation within the influence area of a screw which increases in extreme manner for thinner, less stiff plates can be alleviated in straight forward manner by reduced screw spacings. Very small spacings however render the regarded cramping pressure application technology increasingly less economic. A cramping pressure variation within the bond line area is generally not desirable. However, most important is that the areas with locally reduced pressure are small and that the minimum pressure level in these areas suffices the requirements of the used adhesive. Gap filling properties of specially apt adhesives compensate for inevitable thickness variations in the adherends. For gap filling structural wood adhesives being available today a uniformly distributed cramping pressure level of about 0.2 to 0.5 N/mm² is adequate (e.g. technical approvals [22], [23]) and marks the limits of the base value $p_{nom,req}$ of the cramping pressure requirement for ribbed elements. In order to account for the low pressure locations within the screw influence area the nominal pressure exerted by a screw has to be adjusted by a correction factor $r_{p,min}$ and further by a stress relaxation factor r_{relax}. The pressure verification then reads

$$p_{cramp,eff} = p_{cramp,nom} \cdot r_{relax} \cdot r_{p,min} \leq p_{nom,req} \tag{6}$$

where

$p_{cramp,nom} = F_{ax,k}/A_{screw}$ (with $F_{ax,k}$ acc to Eq. (1) and A_{screw} acc. to Eqs. (4), (5))

$$r_{relax} = 0.75 \quad and \quad r_{p,min} = f(a_1, [EI]_1) = \left(\frac{100}{a_1}\right)^{\sqrt{\left(\frac{230}{(EI)_1}\right)}} \tag{7}$$

with a_1 as screw distance along length axis (1) of the rib in mm, and

$(EI)_1$ bending stiffness in direction 1 in 10^3·kNmm²

Eq. (7) for the minimum pressure ratio $r_{p,min}$ has been derived from the results specified in Table 1 by least square minimization based on prior judgement of an approximation function. Fig. 7 shows the approximation equation (7) graphically. Mechanically more correct ratio $r_{p,min}$, addressing a stress valley, should be expressed as a 2-dimensional quantity, depending on spacings and bending stiffnesses in directions 1 and 2, respectively. However, in a first step this is accounted for, as the here given $r_{p,min}$ values include, as a result of the 3D calculations, implicitly the spacing (actually the edge distance) and plate stiffness in direction 2 orthogonal to the rib axis. So, in case the considered screw configurations do not

deviate significantly from the investigated configurations, $r_{p,min}$ acc. to Eq. (7) can be regarded as a sufficiently accurate estimate for the stress reduction.

7. CONCLUSIONS

The performed numerical investigations with different screw-gluing configurations revealed quantitatively highly variable cramping pressure distributions. The screw spacing and the plate bending stiffness represent the major influencing variables. In multi-row screw applications, a staggered placement of the screws along the rib axis is preferable. Further investigations on several important variables, not addressed here, such as edge distances, rib width, screw head diameter and plates with thicknesses smaller than 60 mm are necessary.

The study revealed that a cramping pressure verification based on an apparent mean value in the screw influence area as specified in ÖNORM B 1995-1-1, includes a significant bias especially in case of CLT plates with thin and medium thicknesses up to about 140 mm. A revised cramping pressure assessment and verification approach is proposed for discussion in the drafting of DIN 1052-10, being presently under revision.

ACKNOWLEDGEMENTS

The partial financial support through innovation program *Zukunft Bau* via Bundesinstitut für Bau-, Stadt und Raumforschung by funding project SWD-10.08.18.7-0.42 “Robotische Schraubenpressklebung: Entwicklung hochleistungs- und anpassungsfähiger, digital geplanter Klebeverbindungen im Holzbau“ is gratefully acknowledged. Further, the presented ongoing research is partially supported by the Deutsche Forschungsgemeinschaft (DFG, German Research Foundation) under Germany's Excellence Strategy - EXC 2120/1 - 390831618.

REFERENCES

[1] ARMBRUSTER, E.: *Einige Probleme bei der Verleimung gerader oder gekrümmter Träger*. In: Mitteilungen der Österreichischen Gesellschaft für Holzforschung 4 (1952), No. 1, pp. 18-21

[2] BRATULIC, K., AUGUSTIN, M., SCHICKHOFER, G.: *Investigations concerning screw-press gluing of assemblies with CLT*. Proceedings International Network on Timber Engineering Research (INTER), Paper: INTER / 52-18-1 (2019), pp. 427-446, Meeting 52, USA

[3] BRATULIC, K., AUGUSTIN, M.: *Screw-Gluing – Theoretical and Experimental Study on Screw Pressure Distribution and Glue Line Strength*, WCTE 2016, Vienna, Austria

[4] BRÜNINGHOFF, H.: *Abklärung der sicherheitstechnisch maßgebenden Faktoren bei der Herstellung von kostensparenden Nagelpressleimungen*, Research Report EGH project E.86/10. Bergische Universität – Gesamthochschule Wuppertal 1991

[5] CHENG, E., SUN, X.: *Effects of wood surface roughness, adhesive viscosity and processing pressure on adhesion strength of protein adhesive*. J. Adhesion Science and Technology 9 (20) (2006), pp. 997-1017

[6] FRANKE, S., SCHIERE, M., FRANKE, B.: *Press Glued Connections - Research Results for Discussion and Standardization*. Proceedings International Network on Timber Engineering Research (INTER), Paper: INTER / 51-18-1, pp. 413-426, Meeting 51, Estonia 2018

[7] RABIEJ, R.J., BEHM, H.D.: *The effect of clamping pressure an orthotropic wood structure on strength of glued bonds*. Wood and Fiber Science 3 (24) (1992), pp. 260-273

[8] RUG, W., GÜMMER, K., GEHRING, S.: *Screw-press bonding with nail screws* (In German). Bautechnik 1 (87) (2010), pp. 33-43

[9] STAPF, G., AICHER, S.: *Pressure Distribution in Block Glue Lines Analyzed by Theory of Beams on Elastic Foundation*. in: Materials and Joints in Timber Structures, RILEM Book series 9 (2014), pp 341-353, Springer

[10] TRUAX, T.R.: *Conditions affecting the making of glued joints*. Research Report. Forest Products Laboratory, US Dept. of Agriculture, Forest Service, Madison, WI, 1924

[11] WASSIPAUL, F.: *Einfluss des Pressdrucks auf die Festigkeit der Leimverbindung bei Brettschichtträgern*. In: Ingenieurholzbau in Forschung und Praxis. Eds. Ehlbeck, J. and Steck, G., pp. 49-54, Bruderverlag Karlsruhe 1982

[12] DIN 1052-10:2012: *Design of timber structures – Part 10: Additional provisions*. German Institute for Standardization (DIN), Berlin

[13] ÖNORM B 1995-1-1:2019: *Eurocode 5: Design of timber structures - Part 1-1: General - Common rules and rules for buildings - Consolidated version with national specifications, national comments and national supplements*

for the implementation of ÖNORM EN 1995-1-1. Austrian Standards International, Vienna

[14] EN 1995-1-1:2004+AC:2006+A1:2008: *Eurocode 5: Design of timber structures – Part 1-1: General-Common rules and rules for buildings.* European Committee for Standardization (CEN), Brussels, Belgium

[15] EN 301:2017: *Adhesives, phenolic and aminoplastic, for load-bearing timber structures. Classification and performance requirements*. European Committee for Standardization (CEN), Brussels

[16] EN 338:2016: Structural timber – Strength classes; European Committee for Standardization (CEN), Brussels

[17] EN 13986:2015: *Wood based panels for use in construction – Characteristics, evaluation of conformity and marking*, European Committee for Standardization (CEN), Brussels

[18] EN 14080:2013: *Timber structures – Glued laminated timber and glued solid timber – Requirements*, European Committee for Standardization (CEN), Brussels

[19] EN 14374:2005: *Timber structures – Structural laminated veneer lumber – Requirements*, European Committee for Standardization (CEN), Brussels

[20] EN 14592:2012: *Timber structures – Dowel-type-fasteners – Requirements*, European Committee for Standardization (CEN), Brussels

[21] Z-9.1-878 (2018) *Technical approval on screw-press gluing by use of HECO-UNIX-top screws* (in German), Approval holder: HECO-Schrauben GmbH & Co.KG, Schramberg, issued by Deutsches Institut für Bautechnik (DIBt), Berlin

[22] Z-9.1-823 (2020): *Technical approval, Melamin-Harnstoffharz-Klebstoff Kauramin Leim 683 mit Kauramin Härter 686 für die Herstellung von geklebten Verbindungen mit dicker Klebstofffuge,* Approval holder: BASF SE Ludwigshafen, issued 15.07.2020 by Deutsches Institut für Bautechnik (DIBt), Berlin

[23] Z-9.1-840 (2019): *Technical approval, Herstellung tragender Holzbauteile und Verklebungen von Verbindungen mit dicker Klebstofffugendicke unter Verwendung des Phenol-Resorcinharz-Klebstoffs Prefere 4094 mit dem Härter Prefere 5827*, Approval holder: Dynea AS, Lillestrom, Norway, issued 22.01.2019 by Deutsches Institut für Bautechnik (DIBt), Berlin